

IBZM tool: a fully automated expert system for the evaluation of IBZM SPECT studies

Ralph Buchert¹, Georg Berding², Florian Wilke¹, Brigitte Martin¹, Daniel von Borczyskowski¹, Janos Mester¹, Winfried Brenner¹, Malte Clausen¹

¹ Department of Nuclear Medicine, University Medical Center Hamburg-Eppendorf, Martinistrasse 52, 20246 Hamburg, Germany

² Department of Nuclear Medicine, University School of Medicine Hannover, Hannover, Germany

Received: 28 July 2005 / Accepted: 12 December 2005 / Published online: 14 April 2006

© Springer-Verlag 2006

Abstract. *Purpose:* Visual reading of [¹²³I]IBZM SPECT scans depends on the experience of the interpreter. Therefore, semi-quantification of striatal IBZM uptake is commonly considered mandatory. However, semi-quantification is time consuming and prone to error, particularly if the volumes of interest (VOIs) are positioned manually. Therefore, the present paper proposes a new software tool (“IBZM tool”) for fully automated and standardised processing, evaluation and documentation of [¹²³I]IBZM SPECT scans.

Methods: The IBZM tool is an easy-to-use SPM toolbox. It includes automated procedures for realignment and summation of multiple frames (motion correction), stereotactic normalisation, scaling, VOI analysis of striatum-to-reference ratio *R*, classification of *R* and standardised display. In order to evaluate the tool, which was developed at the University of Hamburg, the tool was transferred to the University of Hannover. There it was applied to 27 well-documented subjects: eight patients with multi-system atrophy (MSA), 12 patients with Parkinson’s disease (PD) and seven controls. The IBZM tool was compared with manual VOI analysis.

Results: The sensitivity and specificity of the IBZM tool for the differentiation of the MSA subjects from the controls were 100% and 86%, respectively. The IBZM tool provided improved statistical power compared with manual VOI analysis.

Conclusion: The IBZM tool is an expert system for the detection of reduced striatal D₂ availability on [¹²³I]IBZM SPECT scans. The standardised documentation supports visual and semi-quantitative evaluation, and it is useful for presenting the findings to the referring physician. The IBZM tool has the potential for widespread use, since it appears to be fairly independent of the performance

characteristics of the particular SPECT system used. The tool is available free of charge.

Keywords: Parkinsonian syndromes – Dopamine receptors – Single-photon emission computed tomography – ¹²³I-iodobenzamide – IBZM

Eur J Nucl Med Mol Imaging (2006) 33:1073–1083

DOI 10.1007/s00259-006-0067-9

Introduction

Single-photon emission computed tomography (SPECT) imaging with the ¹²³I-labelled raclopride analogue iodobenzamide (IBZM) allows assessment of the availability of postsynaptic dopamine D₂ receptors [1–3]. Common clinical indications are differential diagnosis of parkinsonian syndromes [4–7], assessment of D₂ blockade by neuroleptics [8–11], Huntington’s disease [12] and Wilson’s disease [13]. In addition, [¹²³I]IBZM has been used successfully for the assessment of endogenous dopamine release [14, 15] and for the evaluation of D₂ occupancy by endogenous dopamine [16]. [¹²³I]IBZM SPECT has also been shown to have the potential to become a biological marker for the risk of relapse in alcoholic patients during recovery [17]. [¹²³I]IBZM is known to have suboptimal kinetic properties that are less favourable than those of the PET tracer [¹¹C]raclopride, for example. However, [¹²³I]IBZM is commercially available in Europe and widely used.

Conventional evaluation of [¹²³I]IBZM brain SPECT scans in clinical routine often relies on manual reorientation, visual reading of tomographic slices and semi-quantitative analysis of striatal IBZM uptake using manually defined volumes of interest (VOIs). These steps are time consuming, subjective and prone to error [18]. In addition, a large variety of methods of semi-quantitative analysis are in use, not all of which provide sufficient statistical power [19]. Thus, automatic anatomical standardisation and VOI analysis using standardised predefined

Ralph Buchert (✉)
Department of Nuclear Medicine,
University Medical Center Hamburg-Eppendorf,
Martinistrasse 52,
20246 Hamburg, Germany
e-mail: buchert@uke.uni-hamburg.de
Tel.: +49-40-428036106, Fax: +49-40-428035181

VOIs, as are increasingly used for the evaluation of [^{18}F] fluorodeoxyglucose (FDG) PET brain scans, might be useful for the evaluation of [^{123}I]IBZM brain SPECT scans [20].

Radau et al. described a three-dimensional automated technique for the evaluation of [^{123}I]IBZM SPECT scans [21, 22]. The method focusses on the semi-quantification and voxel-based statistical analysis of striatal IBZM uptake. Visual analysis plays a minor role. However, visual analysis of tomographic slices is essential, not only to check results of the semi-quantitative analysis for plausibility (even in fully automated techniques, errors cannot be ruled out), but also to assess regional distribution of alterations in IBZM uptake.

The present paper proposes a new software tool for fully automated processing, evaluation and documentation of [^{123}I]IBZM SPECT scans with special emphasis on adequate support of visual evaluation. The tool is routinely used to support diagnostic decisions in the departments of nuclear medicine at the University Medical Center, Hamburg and the University School of Medicine in Hannover. Currently it is being implemented at a private nuclear medicine practice in Hamburg.

This study complied with the current German laws, inclusive of ethics approval.

Materials and methods

SPECT imaging procedures used in Hamburg

Prior to imaging, the thyroid gland was blocked by oral administration of perchlorate (600 mg). Then 160–220 MBq [^{123}I]IBZM (GE Healthcare, Braunschweig, Germany) was injected intravenously as a slow bolus (30 s). SPECT imaging was performed about 120 min post injection [23, 24] using a four-head SPECT camera dedicated to brain imaging (Nucline X-Ring/4R, Mediso, Hungary) [25]. The heads of the camera were equipped with low-energy, high-resolution collimators. Patients were positioned on the camera table as comfortably as possible. The head was slightly fixed in a head holder by an elastic gauze bandage around the forehead. A dynamic scan with three consecutive frames (640 s each) was acquired. For each frame, 128 projections, i.e. 32 projections per head, each of 20 s duration, were recorded on a 64×64 matrix with a voxel size of $4.1 \times 4.1 \times 4.1 \text{ mm}^3$. Total acquisition time was 32 min. Total number of counts was about $500 \text{ MBq}^{-1} \text{ min}^{-1}$. Transaxial images were reconstructed iteratively using the ordered subsets-expectation maximisation (OSEM) algorithm of the camera software (16 subsets, 2 iterations). No pre-filtering of the projection data was performed. Reconstructed images were post-filtered using a 3D Butterworth filter (order 5, cut-off 40% of the Nyquist frequency). Spatial resolution of the final images was about 19 mm full-width at half-maximum (FWHM). Attenuation correction was performed using Chang's method with an attenuation coefficient of 0.12 cm^{-1} . No scatter correction was applied. For further processing the format of the reconstructed images was converted from the scanner-specific DIAG format to ANALYZE 7.5 format (Biomedical Imaging Resource, Mayo Foundation) using in-house-developed software.

The three frames were realigned using the Realign tool of the Statistical Parametric Mapping software package (SPM99, Welcome

Department of Cognitive Neurology, Institute of Neurology, University College London, London, UK) [26]. The final uptake image was obtained by summation of the realigned frames.

IBZM template

Twenty consecutive patients from clinical routine in whom [^{123}I]IBZM SPECT had been performed for differential diagnosis of parkinsonian syndromes were recruited retrospectively for the creation of an IBZM template. No specific inclusion or exclusion criteria were applied.

In a first step, each individual IBZM uptake image was stereotactically normalised to the perfusion SPECT template of SPM99 using the Normalise tool of SPM99. In addition to affine transformations, a restricted set of non-linear deformations (warping) was admitted (parameter values for warping: $4 \times 4 \times 4$ non-linear basis functions, 12 non-linear iterations, medium non-linear regularisation, default brain mask, don't mask object). Transformed images were written with a voxel size of $2 \times 2 \times 2 \text{ mm}^3$ using bilinear interpolation. All images were scaled to the same global scale using proportional scaling of SPM99. A preliminary IBZM template was obtained by averaging all images for which normalisation had been successful ($n=12$) (visual assessment using the Check Register Tool of SPM99).

Stereotactic normalisation of all individual IBZM uptake images was repeated, but now using the preliminary IBZM template. An improved preliminary IBZM template was obtained by averaging all images for which this second normalisation had been successful ($n=17$). This procedure was repeated iteratively until stereotactic normalisation was successful in all subjects.

The resulting template was mirrored at the median sagittal plane. Then the original template and the mirrored template were averaged to end up with the final, symmetrical IBZM template (Fig. 1) [27].

Stereotactic normalisation

The uptake image of each individual patient was stereotactically normalised to the IBZM template using the Normalise tool of SPM99 ($4 \times 4 \times 4$ non-linear basis functions, 12 non-linear iterations, medium non-linear regularisation, default brain mask, don't mask object). Transformed images were written with a voxel size of $2 \times 2 \times 2 \text{ mm}^3$ using bilinear interpolation.

Scaling and striatal VOIs

A reference region was obtained from the SPM99 brainmask by generously cutting the striatum in both hemispheres (Fig. 1), i.e. the reference region encompassed all voxels of the brainmask with the exclusion of those of the striatal cavities. The striatal cavities (VOIs) consisted in 13,492 voxels in total, i.e. 6,746 voxels corresponding to about 54 ml on each side.

Scaled uptake images were obtained by dividing each voxel value by the 75th percentile of the voxel values within the reference region.

Semi-quantification

Semi-quantification was performed by hottest voxel analysis [28] of the striata. More precisely, the striatum-to-reference ratio (R) was

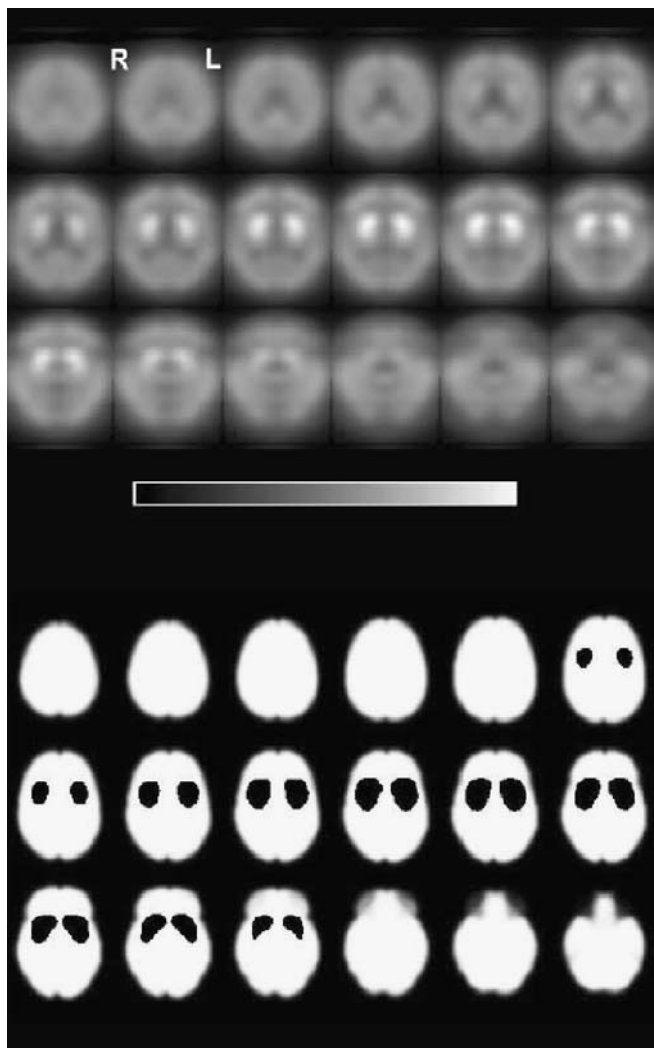


Fig. 1. Transverse slices of the IBZM template (*top*) and the reference region (*bottom*)

estimated separately for each striatum by averaging the scaled uptake values over the 1,875 voxels (15 ml) with the highest scaled uptake within the corresponding striatal VOI.

Normal and pathological range of striatum-to-reference ratio

Since in Hamburg no IBZM SPECT studies in healthy volunteers were available, the normal and pathological range of the striatum-to-reference ratios R were obtained in patients who presumably had a normal R . More precisely, R was obtained in 90 striata of 45 patients (17 females, 28 males, age 61.2 ± 11.1 years) in whom within 2 weeks both ^{123}I -IBZM SPECT and SPECT with the dopamine transporter ligand ^{123}I -FP-CIT (DaTSCAN, GE Healthcare, Braunschweig, Germany) [29] had been performed for diagnosis or exclusion of a parkinsonian syndrome at the University Medical Center, Hamburg. ^{123}I -FP-CIT SPECT images had been evaluated visually (because of the excellent kinetic properties of ^{123}I -FP-CIT, visual evaluation can be considered adequate for the evaluation of ^{123}I -FP-CIT SPECT images).

Assuming that normal FP-CIT uptake in the majority of cases implies normal IBZM uptake, an upper threshold R_P for “pathological” R and a lower threshold R_N for “normal” R were derived from the distribution of R values in those striata in which FP-CIT uptake had been classified as normal visually ($n=27$). R_P was chosen to be the 10th percentile of this distribution, and R_N was chosen to be the lower bound of the 95% confidence limit. This procedure resulted in $R_P=1.40$ and $R_N=1.46$, i.e. $R < 1.40$ was assumed to be pathological and $R > 1.46$ was assumed to be normal. The range $1.40 \leq R \leq 1.46$ was considered as a “grey area”, i.e. inconclusive.

Display (hard copy)

Six transverse slices through the striatum were averaged to one transverse slice of 12 mm thickness. This slice was printed on a black background using a modified continuous spectrum colour table (Fig. 2). A fixed range of scaled uptake values (0.0–1.9) was mapped to the colour table. Uptake values >1.9 were displayed in white (corresponding to uptake =1.9). The upper threshold (1.9) of the domain of the colour table was determined empirically from the mean frequency histogram of scaled uptake values in the visually normal striata that had been used for definition of the normal range of R (Fig. 3). In order to support visual interpretation, typical examples of the same slice in the following findings were displayed on the same page: normal uptake, mildly reduced uptake, severely reduced uptake, and increased uptake.

In addition, a full set of transverse slices at a distance of 4 mm were printed on a separate page using the same colour table.

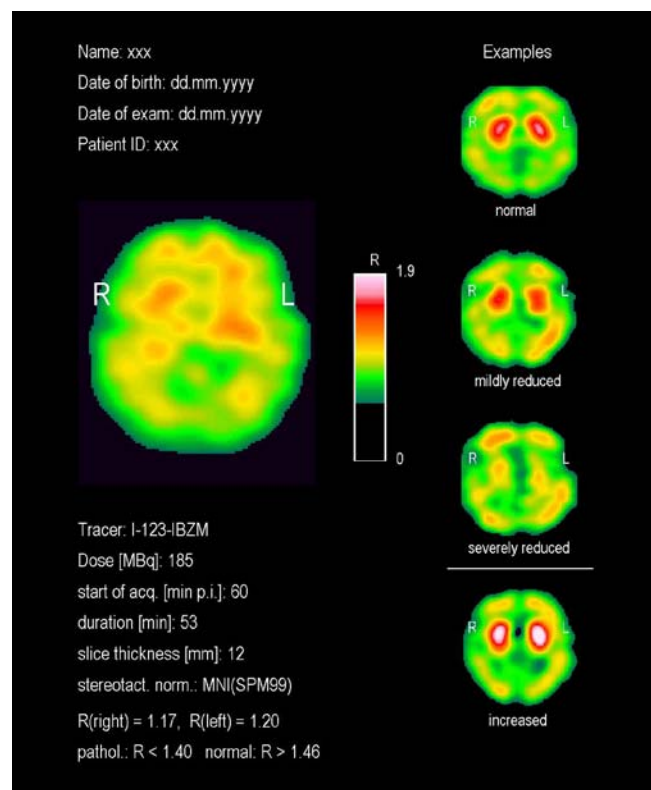


Fig. 2. Documentation page with 12-mm thick slice through the striata. Patient with MSA, confirmed by clinical follow-up (female, 62 years, duration of disease 3 years, Hoehn & Yahr score 3)

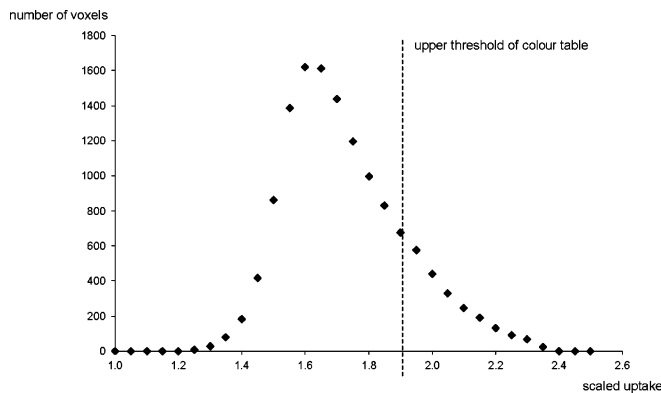


Fig. 3. Histogram of mean frequency of scaled voxel values in visually normal striata in Hamburg patients (cf subsection “Normal and pathological range of striatum-to-reference ratio” in “Materials and methods”)

IBZM tool

Processing (motion correction, stereotactic normalisation, scaling, VOI analysis) and display as described above were integrated into an easy-to-use SPM toolbox (“IBZM tool”).

Hamburg subjects

Sixty-three patients (26 females, 37 males, age 63 ± 11 years) in whom [^{123}I]IBZM SPECT had been performed in Hamburg for differential diagnosis of parkinsonian syndromes were evaluated retrospectively using the IBZM tool.

Visual evaluation versus semi-quantitative evaluation in Hamburg subjects

The images created by the IBZM tool in the 63 Hamburg patients were evaluated by a nuclear medicine technician unaware of the diagnosis and without experience in the evaluation of IBZM SPECT. Using only the documentation page with the thick slice through the striatum (Fig. 2), the technician classified striatal uptake according to the typical examples, i.e. as normal, mildly reduced, severely reduced or increased. The two striata were classified separately. Visual evaluation did not make use of any VOI analysis. Visual evaluation was compared with semi-quantitative evaluation using Spearman correlation analysis (increased=-1, normal=0, mildly reduced=1, severely reduced=2; two-sided test).

Transfer of the IBZM tool to Hannover for external evaluation

Determination of the parameters of the IBZM tool (thresholds for pathological and normal R , colour table) as described above was somewhat empirical. Therefore, the IBZM tool was transferred to the Department of Nuclear Medicine of the University School of Medicine Hannover for external confirmation/evaluation. There are many years of experience with IBZM SPECT in Hannover [30–32].

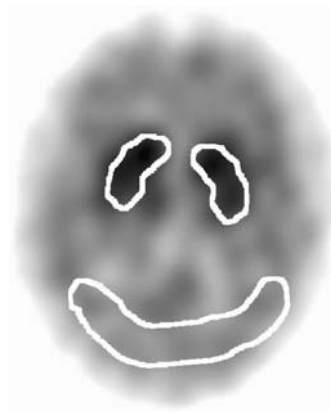


Fig. 4. Standard VOIs used in the manual VOI analysis placed in the summed slice of a control subject from the Hannover sample

SPECT imaging procedures used in Hannover

At the University Medical School, Hannover, IBZM SPECT imaging had been performed according to standard protocols described previously [30, 32]. In short, for data acquisition a Multispect 3 (Siemens, Erlangen, Germany) camera equipped with medium-energy collimators was used. One hundred and eighty projections (60 per head) were acquired using a 1.23 acquisition zoom and a matrix size of 128×128 . The resulting voxel size was $2.9 \times 2.9 \times 2.9 \text{ mm}^3$. Transaxial tomograms were reconstructed using the standard ICON software (Siemens, Erlangen, Germany). Filtered backprojection was performed with a Butterworth filter (cut-off 0.35, order 10). Attenuation correction was done according to Chang assuming a homogeneous attenuation coefficient of $\mu = 0.12 \text{ cm}^{-1}$ within an ellipse drawn around the brain. The relatively low μ value was chosen for implicit scatter correction. Images were then converted to ANALYZE format using the MPI tool (Advanced Tomo Vision ATV, Kerpen, Germany). Reconstructed spatial resolution was about 15 mm.

Hannover subjects

Twenty-seven subjects who had been studied in Hannover previously were included retrospectively: (a) eight patients with probable multi-

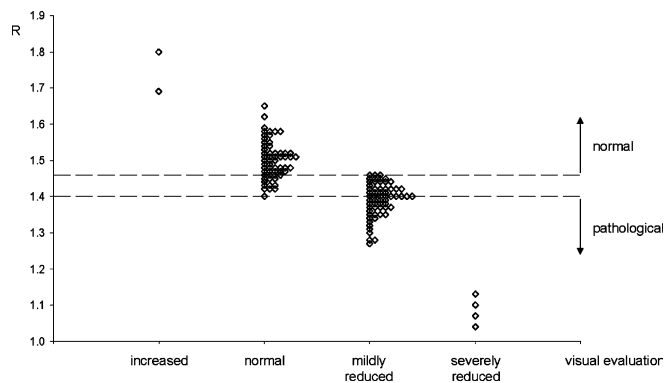


Fig. 5. Striatum-to-reference ratio R versus visual evaluation in 63 Hamburg patients (126 striata) in whom [^{123}I]IBZM SPECT had been performed for differential diagnosis of parkinsonian syndromes

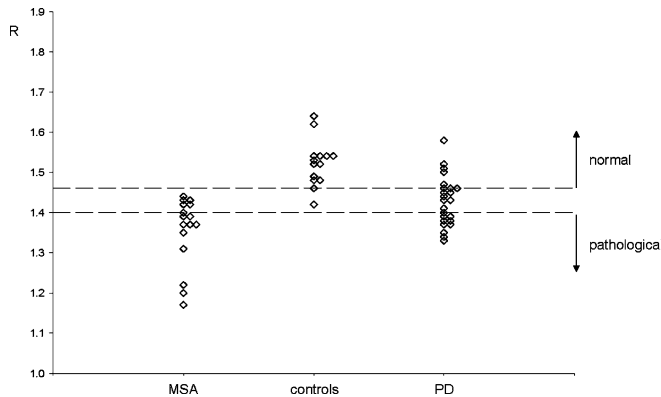


Fig. 6. Striatum-to-reference ratio R in Hannover subjects: eight patients (16 striata) with probable MSA, seven patients (14 striata) without any evidence of neurological disease (controls) and 12 patients (24 striata) with probable idiopathic PD

system atrophy (MSA, six females, two males, age 62 ± 5 years, duration of disease at time of SPECT 2.6 ± 1.6 years, Hoehn-Yahr score 3.3 ± 0.7), (b) 12 patients with advanced (probable) idiopathic Parkinson's disease (PD, five females, seven males, age 58 ± 8 years, duration of disease at time of SPECT 12.5 ± 5.5 years, Hoehn-Yahr score on/off $2.2 \pm 0.9/3.8 \pm 0.7$) and (c) seven control subjects without neurological disease (NC, six females, one male, age 43 ± 17 years). The clinical differential diagnosis of Parkinson syndromes had been fixed by neurologists, specialised in movement disorders, according to established clinical criteria [33, 34]. Medications potentially affecting the dopamine D_2 receptor availability were withdrawn in due time prior to IBZM SPECT according to the guidelines of the European Association of Nuclear Medicine [20].

Adjustment of spatial resolution

Reconstructed spatial resolution of the Hannover images was about 15 mm FWHM (see subsection "SPECT imaging procedures used in Hannover"). In order to adjust the spatial resolution of the Hannover images to the spatial resolution of 19 mm FWHM of the Hannover images, which is the resolution required for the application of the IBZM tool, the Hannover images were smoothed by convolution with an 3D isotropic Gaussian kernel with 12 mm FWHM using the Smooth tool of SPM. No further adjustment was performed.

In general, the required width of the smoothing kernel is given by $\sqrt{19 \times 19 - x \times x}$, where x is the FWHM of the original image in mm.

Evaluation of the IBZM tool in Hannover subjects

The IBZM tool was applied to the 27 Hannover patients.

Statistical analysis of the striatum-to-reference ratio R was performed as follows. First, one-way analysis of variance (ANOVA) and post hoc tests for multiple comparisons were used to compare the groups with respect to R . Scheffé's or Tamhane's post hoc test was applied according to the result of Levene's test of homogeneity of variances. These computations were performed using SPSS 10.0 for MS Windows. In the second step, sensitivity, specificity, positive predictive value and negative predictive value for the differentiation of MSA patients and controls were computed. Two different

thresholds were used: the lower limit R_P and the upper limit R_N of the grey area.

In addition, comparison of visual evaluation and semi-quantitative analysis was performed as described in the subsection "Visual evaluation versus semi-quantitative evaluation in Hamburg subjects".

Manual VOI analysis

In order to further evaluate the potential of the IBZM tool, a non-automatic VOI analysis with manual positioning of fixed VOIs was performed in the 27 Hannover patients.

The original Hannover images, i.e. before adjustment of the spatial resolution for application of the IBZM tool, were manually resliced according to the orbitomeatal line. The four slices with the highest striatal IBZM uptake were summed, resulting in a slice of 11.6 mm thickness. Standard VOIs were positioned on each of both striata and on the occipital cortex on the summed image (Fig. 4). The standard VOIs for the right striatum and the occipital cortex had been manually defined previously in the summed image of one of the Hamburg subjects who had been used for the definition of the normal and pathological range of the striatum-to-reference ratio R . The standard VOI for the left striatum had been obtained by reflecting the right striatum VOI at the mid-sagittal line. The standard VOIs were intended to anatomically delineate the striata and the occipital cortex, and, therefore, were irregular in shape. The surface area of the VOI of one striatum was 5.0 cm^2 ; the surface area of the occipital VOI was 19.0 cm^2 . In consideration of the slice thickness of 11.6 mm, the VOIs represented a volume of 5.8 ml and 22.0 ml, respectively. The standard VOIs were used in all subjects without changes in size and shape. Only the position was adjusted individually by manually shifting and rotating the VOIs until the position appeared optimal visually. The striatum-to-reference ratio was estimated for each striatum separately by the ratio R_m of the average uptake in the striatum VOI and the average uptake in the occipital ROI ("m" indicates manual analysis).

Statistical analysis of group differences in R_m was performed as described in the previous subsection for the IBZM tool's R . R_m and R were compared by Spearman's correlation analysis. In order to check for potential differences in statistical stability between R_m and R , Pitman's test for equality of variances was performed within each of the three groups of subjects [35]. Pitman's test included two steps. First, both R and R_m were scaled to a mean value of 1, separately within each group. Second, a potential correlation between the difference and the sum of scaled R and scaled R_m was analysed by Spearman's correlation test. Significant correlation between difference and sum indicates a significant difference of the coefficient of variance between R_m and R .

Table 1. Semi-quantitative analysis in the Hannover patients (on the basis of striata)

	Pathological ($R < 1.40$)	Inconclusive ($1.40 \leq R \leq 1.46$)	Normal ($1.46 < R$)	Total
MSA	10	6	0	16
Controls	0	2	12	14
PD	9	10	5	24
Total	19	18	17	54

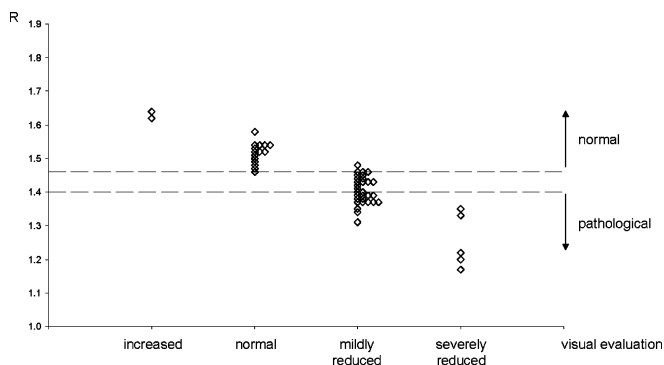


Fig. 7. Striatum-to-reference ratio R versus visual evaluation in the 27 Hannover patients (54 striata)

Results

Automatic stereotactic normalisation was successful in all patients as assessed visually.

The results of the comparison of visual evaluation and semi-quantitative evaluation in 63 subjects from Hamburg are given in the scatter plot in Fig. 5. There was “perfect” correlation, i.e. (a) no striatum which visually was classified as having normal (or increased) uptake had a pathological $R < 1.40$, and (b) no striatum which visually was classified as having reduced (mildly or severely) uptake had a normal $R > 1.46$. This was quantitatively confirmed by the Spearman correlation analysis, which yielded a high correlation with very high statistical significance (correlation coefficient = -0.831 , $p = 0.000$, $n = 126$).

The semi-quantitative results of the IBZM tool in the well-documented Hannover patients are given in Fig. 6. Striatal-to-reference uptake ratio R was 1.36 ± 0.09 ($n = 16$), 1.52 ± 0.06 ($n = 14$) and 1.43 ± 0.06 ($n = 24$) in the MSA group, the control group and the PD group, respectively. The 10th percentile and the lower bound of the 95% confidence limit of R in the control group were 1.44 and 1.49, respectively. Differences between the groups were highly significant according to ANOVA ($df = 53$, $F = 22.165$, $p = 0.000$). Post hoc testing revealed that all groups differed significantly from each other (Levene test: $p = 0.277$; thus Scheffé test: MSA vs controls: $p = 0.000$, MSA vs PD: $p = 0.008$, controls vs PD: $p = 0.001$). None of the MSA patients had normal uptake ratio R , and none of the controls had pathological R (Table 1). Sensitivity, specificity, positive predictive value and negative predictive value for the differentiation of MSA patients from the controls were 63%, 100%, 100% and 70%, respectively, when the lower bound of the grey area was used as the threshold (MSA if $R < R_p = 1.40$), and 100%, 86%, 89% and 100%, respectively, when the upper bound of the grey area was used as the threshold (MSA if $R \leq R_p = 1.46$). Visual analysis showed almost perfect correlation with semi-quantitative evaluation (Fig. 7). Only one striatum (in a control subject) with normal R (1.48) was classified as having mildly reduced uptake visually.

The results of the manual VOI analysis in the Hannover subjects are shown in Fig. 8. The striatum-to-reference ratio

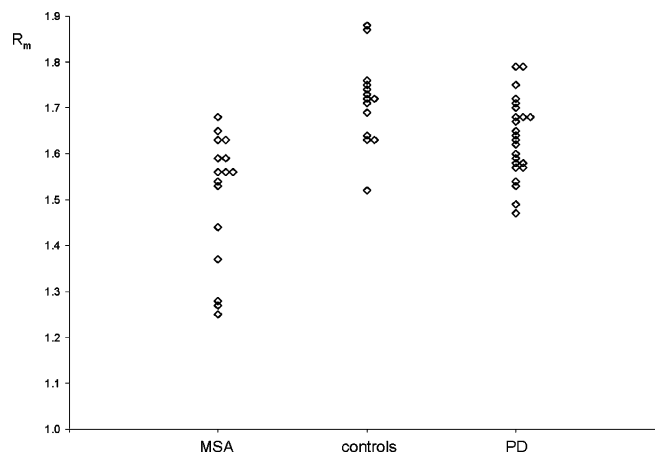


Fig. 8. Manual VOI analysis: Striatum-to-reference ratio R_m in Hannover subjects: eight patients (16 striata) with probable MSA, seven patients (14 striata) without any evidence of neurological disease (controls) and 12 patients (24 striata) with probable idiopathic PD

R_m was 1.51 ± 0.14 ($n = 16$), 1.71 ± 0.09 ($n = 14$) and 1.63 ± 0.09 ($n = 24$) in the MSA, control and PD groups, respectively. R_m showed a highly significant, strong correlation with the IBZM tool's striatum-to-reference ratio R (Spearman correlation coefficient = 0.725 , $p = 0.000$, $n = 54$). The Bland-Altman plot [36] of the difference $R_m - R$ versus the average $0.5 \times (R_m + R)$ given in Fig. 9 revealed (a) that the manual VOI analysis yielded systematically higher values than the IBZM tool (paired t test: $df = 53$, $T = 17.976$, $p = 0.000$) and (b) that the difference increased with increasing striatum-to-reference ratio (Spearman correlation coefficient = 0.490 , $p = 0.000$, $n = 54$). The group effects of R_m were highly significant according to ANOVA ($df = 53$, $F = 14.214$, $p = 0.000$). Post hoc testing revealed that all groups differed significantly from each other (Levene test: $p = 0.040$; thus Tamhane test: MSA vs controls: $p = 0.000$, MSA vs PD: $p = 0.012$, controls vs PD: $p = 0.047$). The scaled striatum-to-reference ratios (scaled to mean value 1 within each group)

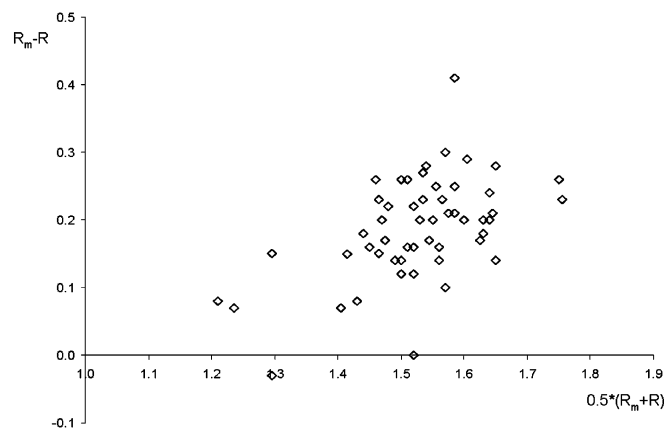


Fig. 9. Bland-Altman plot of the striatum-to-reference ratio estimates of manual VOI analysis (R_m) and fully automated IBZM tool (R) in the 27 Hannover patients (54 striata): difference versus average

had standard deviations 0.063 (R)/0.094 (R_m), 0.038/0.055 and 0.043/0.053 in the MSA, control and PD groups, respectively. While Pitman's test did not reveal a significant difference in the coefficient of variation between the IBZM tool's R and the manual R_m in the PD group (correlation coefficient=0.262, $p=0.217$), there were significant effects in the MSA and control groups (MSA: correlation coefficient=0.676, $p=0.004$; controls: correlation coefficient=0.569, $p=0.034$).

Discussion

In the present paper a new software tool for fully automated standardised processing and documentation of [^{123}I]IBZM SPECT scans is presented (IBZM tool). The IBZM tool includes (a) realignment and summation of multiple frames (motion correction), (b) stereotactic normalisation, (c) scaling, (d) VOI analysis and (e) display.

Dynamic SPECT acquisition allows correction of head movement to some extent, most easily by realignment and summation of the single frames (a more sophisticated method for motion correction of dynamic [^{123}I]IBZM SPECT scans using principle component analysis has been described by Acton et al. [37]). This simple method assumes that movement mainly occurs between frames, and, therefore, in principle works the better the shorter the frames are. However, reduction of frame duration is limited by count statistics. A frame duration of 5 min might be a reasonable compromise (multiple head system). In the present study, frame duration was 10.7 min for reasons of practicability, since the SPECT system (Nucline X-Ring/4R, Mediso, Hungary) did not provide true dynamic acquisition (dynamic acquisition was simulated by performing static scans one after the other).

Spatial resolution of the reconstructed images was about 19 mm FWHM, which appears rather smooth at first sight. However, in a preparatory study (unpublished) we had compared different reconstruction algorithms and filter methods with FWHM between 10 and 20 mm by visual evaluation of the reconstructed images. An FWHM of 19 mm appeared to provide a good compromise between spatial resolution and statistical noise. Smoothing generally reduces the risk of false positive findings, but at the expense of reduced sensitivity. However, a low rate of false positive findings is considered to be useful in a clinical patient care setting.

The spatial resolution of 19 mm FWHM in reconstructed images raises the question of the use of all-purpose (AP) collimators for the acquisition instead of high-resolution (HR) or even ultra-high-resolution (UHR) collimators. The system spatial resolution of an AP collimator is typically about 9 mm FWHM as compared to 7–8 mm for an HR and 6 mm for a UHR collimator, and this difference might not be relevant for a reconstructed resolution of 19 mm. On the other hand, there is a large improvement in sensitivity, by about 50%, when using an AP collimator compared with an HR collimator. This sensitivity gain might be used to reduce the acquisition

time, which is an important factor, particularly in patients with movement disorders and/or dementia. Increased scatter fraction of an AP collimator might be compensated by scatter correction [38]. The effect of different collimators or, more generally, different acquisition and reconstruction protocols, should be addressed more rigorously in further studies.

For stereotactic normalisation an IBZM template was used, since a tracer-specific template in general provides better normalisation results than the standard perfusion template of SPM, for example [39–41]. The IBZM template was created from 20 [^{123}I]IBZM SPECT scans that had been performed for differential diagnosis of parkinsonian syndromes in clinical patient care. No specific inclusion or exclusion criteria were applied. In particular, it was not required that the striatal IBZM uptake was normal in these subjects. The template was intended to be representative of the population of patients referred to our department for IBZM SPECT, in order to avoid unwanted bias by the stereotactic normalisation.

Scaling was performed by dividing each voxel value by the 75th percentile of the voxel values within a predefined mask which basically included the whole brain except the striata (Fig. 1), i.e. the whole brain without the striata was used as the reference region. Other groups have suggested the use of rather small reference regions, the occipital cortex [6], the frontal cortex [12] or the cerebellum [42], for example. The rationale for using these regions was that they might be least affected by neurodegenerative parkinsonian syndromes (in addition to having a very low D_2 density compared with the striatum). However, small reference regions might cause both higher statistical variance and lower reproducibility than large ones. In subjects with neurodegenerative parkinsonian syndrome, IBZM uptake might also be reduced in some extrastriatal brain regions. Scaling using the "whole brain except striata" reference region causes overestimation of the striatum-to-reference ratio R in these subjects. However, this effect is expected to be rather small as long as the affected extrastriatal brain regions do not account for a major part of the whole brain. The situation here is very similar to the situation in brain FDG PET. In brain FDG PET the conventional proportional scaling approach of SPM, which essentially also uses the whole brain or even the whole head as a reference region, has been very successful in the voxel-based statistical evaluation [43]. The IBZM tool attempts to further reduce the effect of putative reduction of IBZM uptake in some extrastriatal brain regions by using the 75th percentile instead of the mean value to characterise IBZM uptake in the reference region. The 75th percentile might be less susceptible to localised extrastriatal alterations of IBZM uptake than the mean.

Striatal IBZM uptake was semi-quantified by hottest voxel analysis within large VOIs predefined in the template such that the whole striata were definitely included (Fig. 1). Hottest voxel analysis within large VOIs might be less sensitive to residual anatomical variations (after stereotactic normalisation) than averaging over all voxels within

anatomically delineated VOIs. The number of hottest voxels to be averaged in each one-sided VOI was chosen to be 1,875, corresponding to a total volume of 15 ml, in order to sample roughly the whole tracer uptake in the striatum. The actual volume of the striatum is about 9 ml and 10 ml in females and males, respectively [44]. The total volume of the hottest voxels was chosen to be slightly larger than the actual volume in order to account for (a) the spatial resolution of the IBZM SPECT images, and (b) the fact that the perfusion SPECT template of SPM and, therefore, also the IBZM template of the IBZM tool, is slightly larger than the average brain. Sampling the whole striatum is important as a neurodegenerative parkinsonian syndrome might not affect the whole striatum. In this case, hottest voxel analysis with a too small number of voxels would be false negative. Acton et al. proposed fuzzy clustering for the automatic segmentation of [^{123}I]IBZM SPECT scans [45]. However, this method requires full dynamic imaging and, therefore, is not applicable in clinical patient care, in which usually only a late static scan is performed.

Striatum-to-reference ratio R ranged from 1.04 to 1.80 in the subjects described in the present paper. This range might appear rather small. However, the standard deviation of R in the Hannover controls was rather small, too (SD=0.06). This suggests that R as estimated by the IBZM tool nevertheless provides significant statistical power for the detection of reduced D_2 availability. This was confirmed by the fact that ANOVA and post hoc testing revealed highly significant R differences between the three Hannover groups, i.e. MSA patients, controls and PD patients.

For visual evaluation the IBZM tool displays a 12-mm-thick transverse slice through the striata using a standardised colour table fixed to a predefined range of scaled uptake values. This ensures that the cortical IBZM uptake is mapped roughly to the 50% value of the colour bar in all subjects, independent of striatal tracer uptake, i.e. the cortex is always displayed with about the same colour. As a consequence, the colour of the striata varies depending on striatal tracer uptake. This is in contrast to the most commonly used individual scaling of the colour bar to the whole range of values within a given study, which causes the striatum, usually the area with the highest uptake, to be always displayed with the maximum colour. Use of the standardised fixed colour table simplifies visual evaluation of [^{123}I]IBZM SPECT scans, as indicated by the “perfect” correlation between semi-quantitative analysis and visual evaluation by an inexperienced interpreter in 63 subjects (126 striata). Thus, semi-quantification is not the only way to objectively assess striatal D_2 availability and it can be vitally supported and critically verified by visual interpretation using an optimised scaling as laid out above.

Parameters of the IBZM tool (thresholds for pathological and normal R , colour table) were fixed somewhat empirically using IBZM SPECT images from Hamburg patients without firmly established diagnoses. For fixing the normal range of R , for example, it was assumed that normal FP-CIT uptake implies normal IBZM uptake. It is well known that this is true in the majority of cases, but

certainly not always. Cases with normal FP-CIT binding but massively impaired IBZM binding have been reported in vascular parkinsonism, for example [46]. Therefore, in order to evaluate the tool and particularly to check the validity of the chosen parameter values, the IBZM tool was transferred to the Department of Nuclear Medicine of the University Medical School, Hannover. In Hannover the IBZM tool was tested rather rigorously using IBZM studies of well-documented patients with clinically confirmed diagnoses and control subjects without evidence of a neurological disease. The good results of this external evaluation confirmed the choice of the parameters of the IBZM tool. The range of normal R and the range of pathological R , for example, were confirmed not only by the high accuracy for the differentiation of MSA subjects and controls, but also by the analysis of the Hannover controls. In fact, applying to the well-documented Hannover controls the same procedure as was used to derive the lower bound R_N of the range of normal R and the upper bound R_P of the range of pathological R from the presumably normal striata in the Hamburg patients yielded values very close to the Hamburg values: $R_N(\text{Hannover})=1.49$ versus $R_N(\text{Hamburg})=1.46$, and $R_P(\text{Hannover})=1.44$ versus $R_P(\text{Hamburg})=1.40$. The fact that the Hannover values were slightly larger than the Hamburg values was most likely due to the difference in age: the Hannover controls were on average 14 years younger than the Hamburg controls (43 ± 17 years vs 57 ± 13 years, unpaired t test: $p=0.042$). Taking into account this age difference and the fact that R is expected to show an age-related decline of about 2.5% per decade in healthy subjects [12], the agreement between the Hannover values and the Hamburg values was excellent. The external confirmation of the parameters of the IBZM tool in the well-documented Hannover sample does provide better evidence for their validity than could have been obtained by additional Hamburg subjects with firmly established diagnosis.

The Hannover SPECT studies had been performed using a different camera, a different acquisition protocol and a different reconstruction algorithm than had been used in Hamburg. The only adaptation applied to the Hannover images was smoothing for adjustment of spatial resolution. The sensitivity, specificity, positive predictive value and negative predictive value of the IBZM tool for the detection of MSA in the Hannover subjects were in good agreement with previous studies. This suggests the validity of the IBZM tool. Simple adjustment of spatial resolution appears sufficient to adapt IBZM scans acquired and processed according to different protocols for analysis with the IBZM tool. In particular, no local adjustment of the bounds of the pathological range and the normal range is required. This simplifies use of the IBZM tool at different institutions.

Limitations of the Hannover patient groups used for the evaluation of the IBZM tool include that (a) control subjects were significantly younger than both MSA and PD subjects (43 ± 17 years vs 62 ± 5 and 58 ± 8 years) and (b) duration of disease was exceptionally long in PD subjects—in particular, it was significantly longer in PD subjects than in MSA subjects (12.5 ± 5.5 years vs 2.6 ± 1.6 years, $p=0.000$).

Concerning effects of age, the striatum-to-reference ratio R is expected to show an age-related decline of about 2.5% per decade in healthy subjects [12]. This effect is rather small and hard to detect in diseased subjects [47]. Therefore, the IBZM tool does not perform an age correction of R . In our departments age is usually used only in difficult cases with inconclusive uncorrected R , i.e. $1.40 \leq R \leq 1.46$ might be diagnosed as normal in “old” patients (≥ 70 years) and as pathological in “young” patients (≤ 40 years).

Concerning the duration of disease, it is well known that there might be compensatory D_2 upregulation in the striatum of patients with early unmedicated PD [42, 48]. PD patients with a long disease duration might also show reduction of postsynaptic D_2 -availability [49]. The Hannover PD patients with a long disease duration were included in the present study for the purpose of confirming the latter possibility, and in fact the IBZM tool revealed pathological R in four of these patients, supporting the hypothesis. This result is a by-product of the present study. It does not allow conclusions to be drawn regarding the potential of the IBZM tool to differentiate between MSA and PD in clinical patient care. Patients referred to IBZM SPECT for differentiation between MSA and PD typically have a much shorter duration of disease than the PD subjects of the Hannover sample included in the present study. The accuracy of the clinical diagnosis increases with the duration of disease, so that nuclear medicine imaging is rarely required in patients with a long disease duration in routine clinical patient care. No patients with a short disease duration and confirmed PD were available in the present study. Therefore, the IBZM tool’s potential to differentiate between short-duration PD and MSA could not be evaluated explicitly. However, it is generally accepted that PD patients with a short disease duration show normal or even slightly increased D_2 availability (cf. above). Therefore, the IBZM tool’s potential to differentiate between short-duration PD and MSA is expected to be the same, or even slightly better, than its potential to differentiate between MSA patients and healthy controls.

The IBZM tool was compared with a standard manual VOI analysis. Although both methods were able to differentiate MSA, control and PD groups of the Hannover sample, the IBZM tool appeared to provide higher levels of statistical significance. The R_m difference of the manual analysis between PD and controls, for example, only just passed the level of statistical significance ($p=0.047$), whereas the R difference of the IBZM tool was highly significant ($p=0.001$). An additional indication of improved statistical power of the IBZM tool compared with manual analysis was provided by Pitman’s test, which demonstrated that the IBZM tool R had a significantly smaller coefficient of variance than the manual R_m , at least in the MSA and control groups.

The IBZM tool is implemented as an SPM toolbox, i.e. the MATLAB (The MathWorks, Inc., Natick, MA, USA)/SPM environment is needed to run the IBZM tool. The IBZM tool can be downloaded free of charge via

anonymous ftp (<ftp://www.ftp.uke.uni-hamburg.de/pub/nuklearmedizin/>). A link will also be given at the SPM homepage (Extensions). The IBZM tool is available for both SPM99 and SPM2. The IBZM tool is easily adapted to local requirements (logo, labelling). The tool requires only that (a) reconstructed IBZM images are given in ANALYZE format and use radiological conventions and (b) spatial resolution is 19 mm FWHM. Detailed online help is provided.

Finally, the IBZM tool is easily adapted to other tracers (SPECT and PET) for the investigation of striatal receptor status. In our departments an analogous tool is used in [^{123}I]FP-CIT SPECT.

In conclusion, the new IBZM tool allows reliable and accurate evaluation of [^{123}I]IBZM SPECT simply by visual interpretation. Based on this new tool, semi-quantification may no longer be the only way to objectively assess striatal D_2 receptor binding. Visual interpretation using optimised scaling can be an excellent supplementary method. This will clearly reduce the reliance of [^{123}I]IBZM SPECT on semi-quantification alone. Even for the experienced interpreter, the IBZM tool might simplify and speed up evaluation of difficult cases. Furthermore, the standardised documentation will assist in presenting easily comprehensible findings to referring physicians.

References

1. Brucke T, Tsai YF, McLellan C, Singhnyom W, Kung HF, Cohen RM, et al. In vitro binding properties and autoradiographic imaging of 3-iodobenzamide ([^{125}I]-IBZM): a potential imaging ligand for D-2 dopamine receptors in SPECT. *Life Sci* 1988;42:2097–2104
2. Costa DC, Verhoeff NP, Cullum ID, Ell PJ, Syed GM, Barrett J, et al. In vivo characterisation of 3-iodo-6-methoxybenzamide [^{123}I] in humans. *Eur J Nucl Med* 1990;16:813–816
3. Kung HF, Alavi A, Chang W, Kung MP, Keyes JW Jr, Velchik MG et al. In vivo SPECT imaging of CNS D-2 dopamine receptors: initial studies with iodine-123-IBZM in humans. *J Nucl Med* 1990;31:573–579
4. Tatsch K, Schwarz J, Oertel WH, Kirsch CM. SPECT imaging of dopamine D2 receptors with [^{123}I]-IBZM: initial experience in controls and patients with Parkinson’s syndrome and Wilson’s disease. *Nucl Med Commun* 1991;12:699–707
5. Schwarz J, Tatsch K, Arnold G, Gasser T, Trenkwalder C, Kirsch CM, et al. [^{123}I]-iodobenzamide-SPECT predicts dopaminergic responsiveness in patients with de novo parkinsonism. *Neurology* 1992;42:556–561
6. van Royen E, Verhoeff NF, Speelman JD, Wolters EC, Kuiper MA, Janssen AG. Multiple system atrophy and progressive supranuclear palsy. Diminished striatal D2 dopamine receptor activity demonstrated by [^{123}I]-IBZM single photon emission computed tomography. *Arch Neurol* 1993;50:513–516
7. Plotkin M, Amthauer H, Klaffke S, Kuhn A, Ludemann L, Arnold G, et al. Combined [^{123}I]-FP-CIT and [^{123}I]-IBZM SPECT for the diagnosis of parkinsonian syndromes: study on 72 patients. *J Neural Transm* 2005;112:677–692
8. Pilowsky LS, Costa DC, Ell PJ, Murray RM, Verhoeff NP, Kerwin RW. Clozapine, single photon emission tomography, and the D2 dopamine receptor blockade hypothesis of schizophrenia. *Lancet* 1992;340:199–202

9. Brucke T, Wober C, Podreka I, Wober-Bingol C, Asenbaum S, Aull S, et al. D2 receptor blockade by flunarizine and cinnarizine explains extrapyramidal side effects. A SPECT study. *J Cereb Blood Flow Metab* 1995;15:513–518
10. Tauscher J, Kufferle B, Asenbaum S, Tauscher-Wisniewski S, Kasper S. Striatal dopamine-2 receptor occupancy as measured with [¹²³I]iodobenzamide and SPECT predicted the occurrence of EPS in patients treated with atypical antipsychotics and haloperidol. *Psychopharmacology (Berl)* 2002;162:42–49
11. la Fougere C, Meisenzahl E, Schmitt G, Stauss J, Frodl T, Tatsch K et al. D2 receptor occupancy during high- and low-dose therapy with the atypical antipsychotic amisulpride: a ¹²³I-iodobenzamide SPECT study. *J Nucl Med* 2005;46:1028–1033
12. Brucke T, Podreka I, Angelberger P, Wenger S, Topitz A, Kufferle B, et al. Dopamine D2 receptor imaging with SPECT: studies in different neuropsychiatric disorders. *J Cereb Blood Flow Metab* 1991;11:220–228
13. Oertel WH, Tatsch K, Schwarz J, Kraft E, Trenkwalder C, Scherer J, et al. Decrease of D2 receptors indicated by ¹²³I-iodobenzamide single-photon emission computed tomography relates to neurological deficit in treated Wilson's disease. *Ann Neurol* 1992;32:743–748
14. Laruelle M, Abi-Dargham A, van Dyck CH, Gil R, D'Souza CD, Erdos J, et al. Single photon emission computerized tomography imaging of amphetamine-induced dopamine release in drug-free schizophrenic subjects. *Proc Natl Acad Sci USA* 1996;93:9235–9240
15. Booij J, Korn P, Linszen DH, van Royen EA. Assessment of endogenous dopamine release by methylphenidate challenge using iodine-123 iodobenzamide single-photon emission tomography. *Eur J Nucl Med* 1997;24:674–677
16. Laruelle M, D'Souza CD, Baldwin RM, Abi-Dargham A, Kaner SJ, Fingado CL et al. Imaging D2 receptor occupancy by endogenous dopamine in humans. *Neuropsychopharmacology* 1997;17:162–174
17. Guardia J, Catafau AM, Batlle F, Martin JC, Segura L, Gonzalvo B, et al. Striatal dopaminergic D₂ receptor density measured by [¹²³I]iodobenzamide SPECT in the prediction of treatment outcome of alcohol-dependent patients. *Am J Psychiatry* 2000;157:127–129
18. Verhoeff NP, Kapucu O, Sokole-Busemann E, van Royen EA, Janssen AG. Estimation of dopamine D2 receptor binding potential in the striatum with iodine-123-IBZM SPECT: technical and interobserver variability. *J Nucl Med* 1993;34:2076–2084
19. Hertel A, Weppner M, Baas H, Schreiner M, Maul FD, Baum RP, et al. Quantification of IBZM dopamine receptor SPET in de novo Parkinson patients before and during therapy. *Nucl Med Commun* 1997;18:811–822
20. Tatsch K, Asenbaum S, Bartenstein P, Catafau A, Halldin C, Pilowsky LS, et al. European Association of Nuclear Medicine procedure guidelines for brain neurotransmission SPET using ¹²³I-labelled dopamine D₂ receptor ligands. *Eur J Nucl Med Mol Imaging* 2002;29:BP23–BP29
21. Radau PE, Linke R, Slomka PJ, Tatsch K. Optimization of automated quantification of ¹²³I-IBZM uptake in the striatum applied to parkinsonism. *J Nucl Med* 2000;41:220–227
22. Popperl G, Radau P, Linke R, Hahn K, Tatsch K. Diagnostic performance of a 3-D automated quantification method of dopamine D2 receptor SPECT studies in the differential diagnosis of parkinsonism. *Nucl Med Commun* 2005;26:39–43
23. Verhoeff NP, Brucke T, Podreka I, Bobeldijk M, Angelberger P, Van Royen EA. Dynamic SPECT in two healthy volunteers to determine the optimal time for in vivo D2 dopamine receptor imaging with ¹²³I-IBZM using the rotating gamma camera. *Nucl Med Commun* 1991;12:687–697
24. Gutzki J, Martin B, Wilke F, Buchert R, Mester J, Clausen M. Time dependence of striatum to background ratio in 123-I-IBZM SPET. *Eur J Nucl Med Mol Imaging* 2003;30:S157
25. Buchert R, Mester J, Bohuslavizki KH, Clausen M. Performance characteristics of a new low-cost four-headed small-field-of-view gamma camera dedicated for brain imaging. *J Nucl Med* 2001;42:886
26. Friston KJ, Holmes AP, Worsley KJ, Poline JP, Frith CD, Frackowiak RSJ. Statistical parametric maps in functional imaging: a general linear approach. *Hum Brain Mapp* 1995;2:189–210
27. Larisch R, Meyer W, Klimke A, Kehren F, Vosberg H, Muller-Gartner HW. Left-right asymmetry of striatal dopamine D2 receptors. *Nucl Med Commun* 1998;19:781–787
28. Duarte P, Hustinx R, Couturier O, Smith RJ, Alavi A. Hottest pixel analysis: useful value or statistical artifact? *J Nucl Med* 1999;40:292P
29. Kuikka JT, Bergstrom KA, Ahonen A, Hiltunen J, Haukka J, Lansimies E, et al. Comparison of iodine-123 labelled 2 beta-carbomethoxy-3 beta-(4-iodophenyl)tropane and 2 beta-carbomethoxy-3 beta-(4-iodophenyl)-N-(3-fluoropropyl)nortropane for imaging of the dopamine transporter in the living human brain. *Eur J Nucl Med* 1995;22:356–360
30. Berding G, Gratz KF, Kolbe H, Meyer GJ, Dengler R, Knoop BO, et al. ¹²³I-IBZM SPECT: reconstruction methodology and results in parkinsonism and dystonia. *Nuklearmedizin* 1994;33:194–199
31. Weissenborn K, Berding G, Kostler H. Altered striatal dopamine D2 receptor density and dopamine transport in a patient with hepatic encephalopathy. *Metab Brain Dis* 2000;15:173–178
32. Muller-Vahl KR, Berding G, Kolbe H, Meyer GJ, Hundeshagen H, Dengler R, et al. Dopamine D2 receptor imaging in Gilles de la Tourette syndrome. *Acta Neurol Scand* 2000;101:165–171
33. Gelb DJ, Oliver E, Gilman S. Diagnostic criteria for Parkinson disease. *Arch Neurol* 1999;56:33–39
34. Gilman S, Low PA, Quinn N, Albanese A, Ben-Shlomo Y, Fowler CJ, et al. Consensus statement on the diagnosis of multiple system atrophy. *J Neurol Sci* 1999;163:94–98
35. Armitage P, Berry G. *Statistical methods in medical research*, 3rd edn. Malden, USA: Blackwell Science Ltd; 1998
36. Bland JM, Altman DG. *Statistical methods for assessing agreement between two methods of clinical measurement*. *Lancet* 1986;1:307–310
37. Acton PD, Pilowsky LS, Suckling J, Brammer MJ, Ell PJ. Registration of dynamic dopamine D2 receptor images using principal component analysis. *Eur J Nucl Med* 1997;24:1405–1412
38. Nikkinen P, Liewendahl K, Savolainen S, Launes J. Validation of quantitative brain dopamine D2 receptor imaging with a conventional single-head SPET camera. *Eur J Nucl Med* 1993;20:680–683
39. Meyer JH, Gunn RN, Myers R, Grasby PM. Assessment of spatial normalization of PET ligand images using ligand-specific templates. *Neuroimage* 1999;9:545–553
40. Gispert JD, Pascau J, Reig S, Martinez-Lazaro R, Molina V, Garcia-Barreno P, et al. Influence of the normalization template on the outcome of statistical parametric mapping of PET scans. *Neuroimage* 2003;19:601–612
41. Van Laere K, Koole M, D'Asseler Y, Versijpt J, Audenaert K, Dumont F, et al. Automated stereotactic standardization of brain SPECT receptor data using single-photon transmission images. *J Nucl Med* 2001;42:361–375
42. Laulumaa V, Kuikka JT, Soininen H, Bergstrom K, Lansimies E, Riekkinen P. Imaging of D2 dopamine receptors of patients with Parkinson's disease using single photon emission computed tomography and iodobenzamide I 123. *Arch Neurol* 1993;50:509–512

43. Stamatakis EA, Glabus MF, Wyper DJ, Barnes A, Wilson JT. Validation of statistical parametric mapping (SPM) in assessing cerebral lesions: A simulation study. *Neuroimage* 1999;10: 397–407
44. Jenkins TW, Truex RC. Dissection of the human brain as a method for its fractionation by weight. *Anat Rec* 1963;147: 359–366
45. Acton PD, Pilowsky LS, Kung HF, Ell PJ. Automatic segmentation of dynamic neuroreceptor single-photon emission tomography images using fuzzy clustering. *Eur J Nucl Med* 1999;26:581–590
46. Plotkin M, Amthauer H, Quill S, Marzinzik F, Klostermann F, Klaffke S, et al. Imaging of dopamine transporters and D2 receptors in vascular parkinsonism: a report of four cases. *J Neural Transm* 2005;112:1355–1361
47. Parellada E, Lomena F, Catafau AM, Bernardo M, Font M, Fernandez-Egea E, et al. Lack of sex differences in striatal dopamine D2 receptor binding in drug-naive schizophrenic patients: an IBZM-SPECT study. *Psychiatry Res* 2004;130: 79–84
48. Wenning GK, Donnemiller E, Granata R, Riccabona G, Poewe W. ^{123}I -beta-CIT and ^{123}I -IBZM-SPECT scanning in levodopa-naive Parkinson's disease. *Mov Disord* 1998;13:438–445
49. Hwang WJ, Yao WJ, Wey SP, Shen LH, Ting G. Down-regulation of striatal dopamine D2 receptors in advanced Parkinson's disease contributes to the development of motor fluctuation. *Eur Neurol* 2002;47:113–117